J Wood Sci (2011) 57:276–281
DOI 10.1007/s10086-011-1174-1

ORIGINAL ARTICLE

Akio Koizumi · Keisuke Ikeda · Kei Sawata
Takuro Hirai

Nondestructive measurement of cross-sectional shape of a tree trunk

Received: August 26, 2010 / Accepted: January 17, 2011 / Published online: May 20, 2011

Abstract To evaluate windthrow resistance with respect to stem breakage, a nondestructive method for determining the shape of trunk cross sections was developed. In this method, the coordinates of multiple gauge points set on the perimeter of a trunk are calculated by measuring the distances between them. The shape between the gauge points is generated with the use of a profile gauge placed between them. Measurement tests were conducted using profile gauges with lengths of 300 and 900 mm on model specimens with four shape patterns and four different diameters. The accuracy of the estimation was verified by comparing the section modulus calculated for the generated image and for the photograph. The average ratio of section modulus (generated/photo) for all specimens was 0.994, which indicates that the proposed method is highly accurate. The section moduli of hollow trunks can be evaluated using the profile method together with the drill resistance technique on the condition that 26% of the trunk diameter could be drilled without skew.

Key words Nondestructive evaluation · Section modulus · Windthrow resistance · Tree trunk · Drill resistance technique

Introduction

When analyzing windthrow resistance of standing trees, trees can be considered as cantilevered beams that are supported by a root plate in the ground. The load induced by a storm wind force acting on the tree crown can cause breakage of the trunk or uprooting. Although the common cause of stem breakage is bending failure, shear failure[1] and shell buckling[2] also play a role in the case of thin-walled trunks that suffer from heartwood decay. Regardless of which failure mechanism applies, accurate measurement of the shape of the cross section at a critical height of the trunk is required.

The cross section of the trunks of well-conditioned plantation-grown conifers can be assumed to be circular. However, roadside or park trees are often aged or injured and the cross section of such tree trunks may be irregular and hollowed. In order to evaluate the moment of inertia and the section modulus of irregular cross sections, a computing method using binarized images of the shape of cross sections was developed and applied to the estimation of the critical wind speed for aged poplar trees with hollow trunks.[3] However, the binarized images were converted from photographs of the crosscut surface taken after the trees were felled – a method that is inappropriate for the diagnosis of windthrow hazard. Consequently, this study considers a nondestructive method of measuring the outside shapes of tree trunks that uses a profile gauge.

To perform nondestructive estimation of the distribution of decay or hollowed areas inside trunks, it is possible to apply X-ray-computed tomography.[4] However, the devices developed for this purpose are not sufficiently portable and thus could not be used for in situ diagnosis.[5] Although computed tomography using stress waves or ultrasonic waves have been developed[6], the accurate evaluation of sound wood thickness is difficult, especially for trees less than 1 m in diameter.[7] The thickness of sound sapwood has been measured by a drilling device using a drill resistance technique.[8] Since the diameter of the fine drill employed is as small as 3 mm, the damage to the tree is considered negligible. This drilling resistance technique has been used for the detection of heartwood decay in park trees[7] and for the inspection of exterior structures such as wooden bridges.[9] The purpose of this study was to propose a nondestructive method of estimating the cross-sectional shape of trees for windthrow risk analysis.

A. Koizumi (✉) · K. Ikeda · K. Sawata · T. Hirai
Graduate School of Agriculture, Hokkaido University, N9 W9, Sapporo 060-8589, Japan
Tel. +81-11-706-3340; Fax +81-11-706-3636
e-mail: akoizumi@for.agr.hokudai.ac.jp

Part of this study was presented at the 60th Annual Meeting of the Japan Wood Research Society in Miyazaki, March 2010

Materials and methods

Measurement of outside shape of a trunk using a profile method

After establishing the gauge points on the perimeter of a tree trunk in the horizontal plane (points A–E in Fig. 1), the distance from point A to each gauge point and the distance between adjacent points were measured with a caliper. Then the coordinates of the gauge points (X, Y) and the angles the lines make with the X axis (β) were determined. With reference to triangle ABC in Fig. 1, the angles of line AC from the X axis (α) and line BC from the X axis (β) can be calculated using the height of the triangle (h), with the longest side as the base.

$$h = \frac{2A}{\max(a, b, c)} \tag{1}$$

Where $A = \sqrt{s(s-a)(s-b)(s-c)}$, $s = \frac{(a+b+c)}{2}$ (Heron's formula)

$$\alpha = \begin{cases} \sin^{-1}\dfrac{h}{c} & a = \max(a, b, c) \\ \pi - \left(\sin^{-1}\dfrac{h}{a} + \sin^{-1}\dfrac{h}{c}\right) & b = \max(a, b, c) \\ \sin^{-1}\dfrac{h}{a} & c = \max(a, b, c) \end{cases} \tag{2}$$

$$\beta = \begin{cases} \pi - \sin^{-1}\dfrac{h}{b} & a = \max(a, b, c) \\ \pi - \sin^{-1}\dfrac{h}{a} & b = \max(a, b, c) \\ \pi - \left(\cos^{-1}\dfrac{h}{a} + \cos^{-1}\dfrac{h}{b}\right) & c = \max(a, b, c) \end{cases} \tag{3}$$

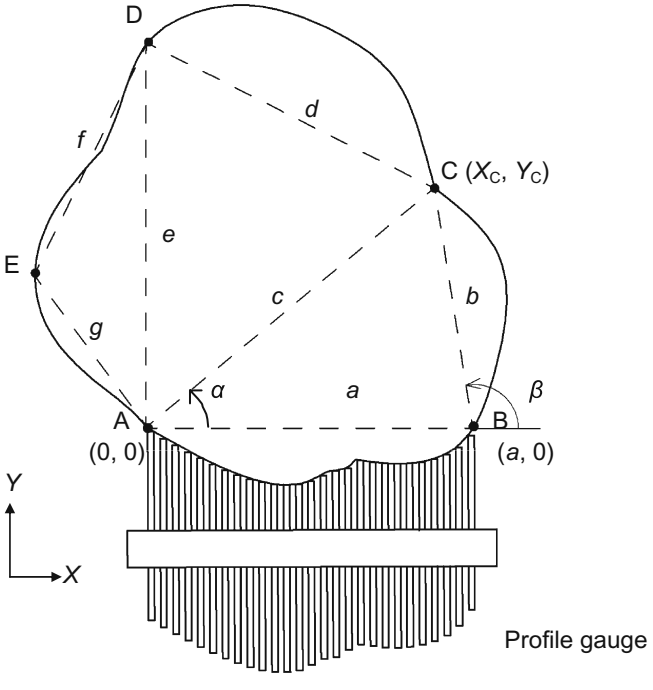

Fig. 1. Profile method for measurement of outside shape of a tree trunk

Then the coordinates of point C (X_C, Y_C) can be determined from α and c.

$$X_C = c\cos\alpha \tag{4}$$

$$Y_C = c\sin\alpha \tag{5}$$

X_C, Y_C, and β in Fig. 1 are expressed by Eqs. 6–8, derived by substituting Eqs. 1 and 2 into Eqs. 4 and 5 and rearranging:

$$X_C = \begin{cases} -c\cos\left(\sin^{-1}\dfrac{2A}{ab} + \sin^{-1}\dfrac{2A}{bc}\right) & b = \max(a, b, c) \\ c\sqrt{1 - \dfrac{4A^2}{a^2c^2}} & b \neq \max(a, b, c) \end{cases} \tag{6}$$

$$Y_C = \begin{cases} c\sin\left(\sin^{-1}\dfrac{2A}{ab} + \sin^{-1}\dfrac{2A}{bc}\right) & b = \max(a, b, c) \\ \dfrac{2A}{a} & b \neq \max(a, b, c) \end{cases} \tag{7}$$

$$\beta = \begin{cases} \pi - \left(\cos^{-1}\dfrac{2A}{ac} + \cos^{-1}\dfrac{2A}{bc}\right) & c = \max(a, b, c) \\ \pi - \sin^{-1}\dfrac{2A}{ab} & c \neq \max(a, b, c) \end{cases} \tag{8}$$

The coordinates for the rest of the gauge points are calculated in the same manner, creating an image with a polygonal shape (Fig. 1). After fitting a profile gauge to each interval between adjacent gauge points, line segments that were extracted from digital photographs of the fitted profile gauge were pasted to the sides of the polygon. An example of the generated outside shape with a polygon and a photograph of a stump cross section are shown in Fig. 2. The xylem cross section can be estimated by subtracting the bark thickness from the outside shape.

Two profile gauges were used in this study: one was a commercially produced gauge with a 300-mm span (needle pitch: 1 mm) and the other was made of lumber and aluminum pipes (span: 900 mm, needle pitch: 10 mm) (Fig. 3).

Verification of accuracy of outside shape estimation

Although the cross-sectional shapes of tree trunks are regularly circular or oval, aged trees tend to have irregular shape with multiple limbs. Considering the shapes of aged park

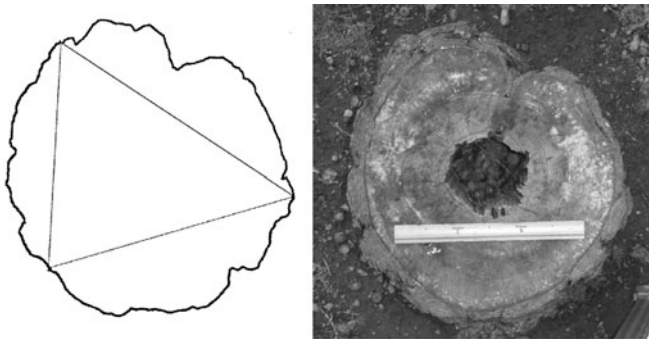

Fig. 2. Example of the generated outside shape of a stump (*left*) and photograph (*right*)

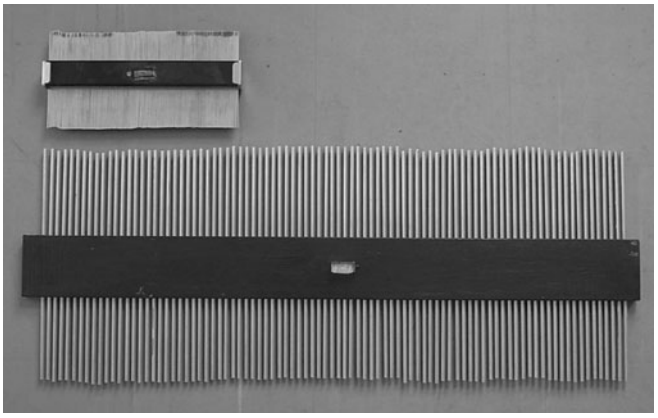

Fig. 3. Profile gauges: *upper*, 300-mm span with 1-mm pitch; lower, 900-mm span with 10-mm pitch

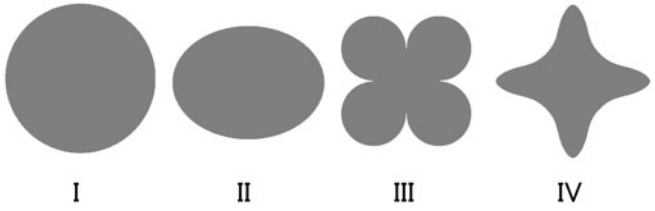

Fig. 4. Outside shape patterns of the specimens. Section moduli for patterns I, II, III, and IV, 1 m in diameter, were calculated using Eq. 9 as 0.0982, 0.0553, 0.0698, and 0.0281 m^3, respectively.

trees, shape patterns I–IV (Fig. 4) were chosen to verify the accuracy of outside shape estimation. The specimens were cut with a jigsaw from 40-mm-thick side-jointed dimension lumber. Specimens of four sizes (300, 600, 900, and 1200 mm in maximum diameter) were made for each shape pattern. Measurement testing was conducted using two profile gauges and three repetitions for each specimen. A photograph of the outside shape was taken for each specimen for later verification.

Verification was performed by comparing the section modulus (Z) as calculated using the bitmap image determined from the current profile method with the Z value converted from the photograph of each specimen. The Z values were numerically calculated from Eq. 9 by scanning the bitmap images[3]:

$$Z = \frac{\Sigma(y-\lambda_1)^2 \mathrm{d}A}{\max(\lambda_1, \lambda_2)} \quad (9)$$

where $\lambda_1 = \frac{\Sigma y \mathrm{d}A}{\Sigma \mathrm{d}A}$, $\lambda_2 = L_y - \lambda_1$ (see Fig. 5).

The bitmap images were rotated 0°, 45°, 90°, and 135° and four Z values were obtained. Then the four Z values were averaged for each bitmap image.

Inspection for skew of the needle during drilling

For a trunk with heartwood decay, the thickness of sound sapwood can be estimated using the drill resistance technique.[8] It has been reported, however, that the fine drilling needle (with a shank diameter of 1.5 mm) was apt to be skewed when drilling deep into the wood.[7,10] If this is the case, it may be difficult to obtain an accurate measurement of the sound xylem thickness. To better understand the skew of a drilling needle, a series of drilling tests was conducted. Specimens were cut from logs of *Robinia pseudoacacia* and *Fraxinus excelsior* (Table 1). It was considered that these species were likely to induce skew because of the high wood density and the large variations in density within a growth ring. The logs were approximately 500 mm long. Planks with a thickness of 50 mm and a width of 300 mm, including pith cut from the logs, were held to the drilling device (IML-RESI F500) with clamps. The drill-holes were located at three points in a line 20 mm away from the end surface (Fig. 6). The drilling was conducted from the bark-side surface along the radial direction toward the pith. After the test, the

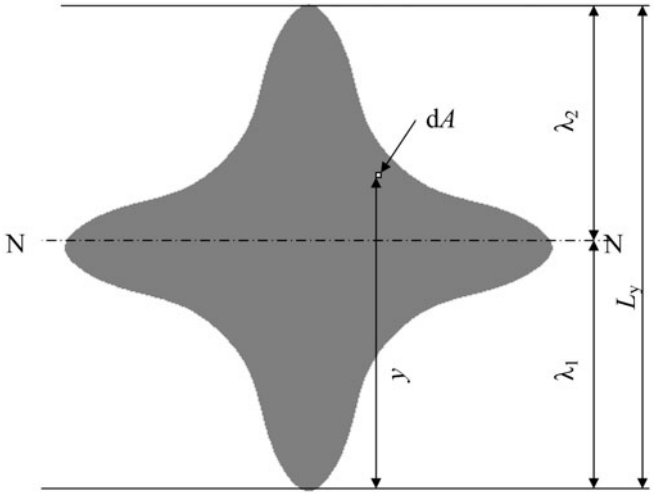

Fig. 5. Definitions of parameters used in calculation of section modulus (Z). N–N denotes the neutral axis; dA is a pixel of the bitmap image

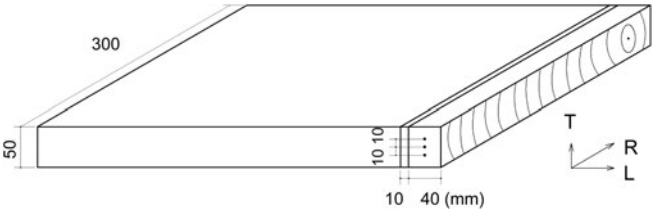

Fig. 6. Sample plank for inspecting skew of the drilling needle. T, R, and L refer to the tangential, radial, and longitudinal directions, respectively

Table 1. Wood density and average ring width of specimens for drilling test

Species	Log diameter (mm)	Air-dry density (kg/m^3)	Average ring width (mm)
RP	826	724	11.4
FE	950	701	8.8

RP, *Robinia pseudoacacia*; FE, *Fraxinus excelsior*

specimens were crosscut 40 mm from the end surface. Each specimen was sliced at 10-mm intervals from the bark-side tangential face in order to follow the tracks of the drill holes. Deviations (absolute values) of the drill holes in the longitudinal and tangential directions were measured for these 40×50 mm areas of the sliced pieces. Then a 10-mm-thick specimen was crosscut from the rest of the plank in order to measure the moisture content at the drilling test site. The drilling test was conducted three times for each plank during conditioning of the moisture content from a moist condition to an air-dry condition in a humidity chamber.

Inspection for the effect of hollow size on section modulus calculation

Inner cavities and heartwood decay reduce the section modulus and weaken the resistance to stem breakage. Deep drilling is necessary to measure the sound xylem thickness in the case of large aged trees, which may result in inaccurate evaluation of xylem thickness due to the skew of the drilling needle. However, the effect of a hollow located near the pith is known to be small. The effect of the size of the hollow part on the section modulus was inspected by numerical analysis[3] using the bitmap images of shape patterns I–IV with hollows of 10% to 90% of the outside diameter.

Results and discussion

The effects of shape patterns and specimen size on the error in section modulus estimation

The ratio of the Z value calculated for the generated image of the outside shape of specimens using the profile method to that calculated for the image converted from photographs of the specimens was compared for various shape patterns and specimen sizes.

With regard to the shape pattern, errors were comparatively large for patterns III and IV; the average Z ratios were 1.03 (pattern III) and 0.96 (pattern IV) and the variations were rather large for those patterns. The number of gauge points required for patterns III and IV was greater than those for patterns I and II, especially when using the 300-mm gauge (Table 2). The variations of the Z ratios for which a 300-mm gauge was used were greater than those for which 900-mm gauge was used, except for pattern IV. These results suggest that the use of a short-span gauge to measure a complicated shape would require a higher number of gauge points and would generate a cumulative error in calculating the coordinates of the gauge points.

As regards the relationship between specimen size and error in Z estimation, the variation was large for a specimen size of 1200 mm (Fig. 7). It was suspected that the number of gauge points had some effect on the accumulation of errors in coordinate calculation (Table 2). The variation for the 1200-mm specimen using a 300-mm gauge was greater than it was using a 900-mm gauge. On the other hand, the variation for a specimen size of 300 mm using a 900-mm gauge was greater than it was for a 300-mm gauge. This result may be attributed to the roughness of the profiling obtained using a 900-mm gauge with a 10-mm needle pitch compared with the specimen size. The average Z ratio for all conditions was 0.994, which showed the high accuracy of Z estimation achieved by the proposed profile method.

Table 2. Number of required gauge points for test conditions

Specimen size (mm)	Pattern I		Pattern II		Pattern III		Pattern IV	
	300	900	300	900	300	900	300	900
300	3	3	3	2	4	4	4	2
600	6	3	5	2	8	4	8	2
900	10	3	8	3	12	4	10	4
1200	13	4	12	4	16	5	12	4
Average	8.0	3.3	7.0	2.8	10.0	4.3	8.5	3.0

Patterns I–IV are shown in Fig. 4. The values of 300 and 900 beneath the pattern numbers are the length of the profile gauges in mm

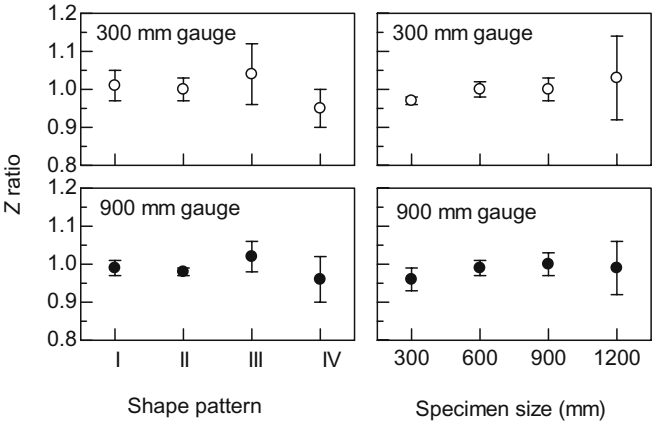

Fig. 7. Z ratios for different shape patterns and specimen sizes using 300-mm and 900-mm profile gauges. The Z ratio is the ratio of the section modulus calculated for the generated image using the profile method to that calculated for the image converted from the photograph. *Error bars* denote standard deviations

Skew of the needle during drilling operation

The average moisture content for the three drilling test runs was 48%, 22%, and 13% and 49%, 21%, and 9% for the *Robinia* and *Fraxinus* specimens, respectively. The drilling needle was skewed such that it stuck out from the plank surface in a number of the test runs. Because the emergence of the needle was observed at distances of more than 210 mm from the bark-side edge, we analyzed the trajectories up to 210 mm for the test runs that showed the maximum deviation among three drill holes (Fig. 8) and the average and maximum value of the deviation at a depth of 210 mm (Table 3).

There was no significant difference between the drill-hole deviation in the longitudinal and tangential directions at a depth of 210 mm; the t value calculated using Student's t test was 0.052. Although differences in drilling resistance

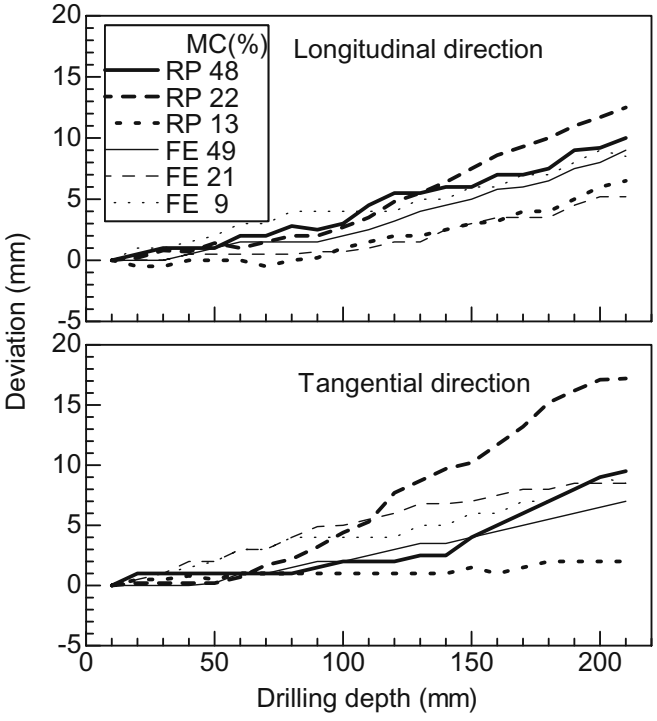

Fig. 8. Deviations of drilling hole associated with drilling depth for various moisture contents (*MC*). RP, *Robinia pseudoacacia*; FE, *Fraxinus excelsior*

Table 3. Skew deviation of the drilling needle at a depth of 210 mm from bark-side surface

Species	MC (%)	Deviation-L (mm)		Deviation-T (mm)	
		Average	Maximum	Average	Maximum
RP	48	6.3	10.0	5.0	9.5
RP	22	9.1	12.5	10.6	17.2
RP	13	4.8	6.5	1.0	2.0
FE	49	6.3	9.5	4.2	7.0
FE	21	3.7	5.2	7.8	8.5
FE	9	5.7	8.5	4.2	7.0

Deviation-L and -T denotes the skew (absolute value) in the longitudinal and tangential directions, respectively (see Fig. 6) MC, moisture content

at deep locations have been observed between green wood and air-dry wood[11], no difference in deviation was recognized between the moist condition (beyond the fiber saturation point) and air-dry condition in this set of experiments (t value was 0.362). The maximum deviations at a depth of 210 mm were 12.5 mm for the longitudinal direction and 17.2 mm for the tangential direction. A 20-mm deviation at a depth of 210 mm would give a secant gradient of 0.095 rad, so that the error in estimating the xylem thickness would be 0.5%, which is negligible.

Effect of hollow trunks on reduction in section modulus

Bitmap images of patterns I–IV with hollows that have the same shape as the outside shape for various hollow sizes

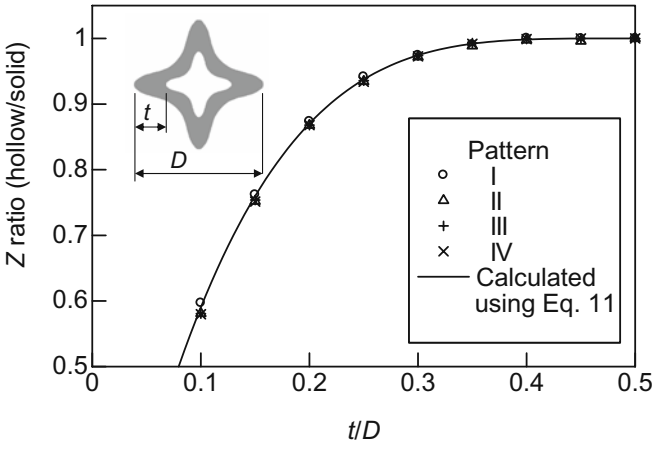

Fig. 9. Relationship between t/D and Z ratio. t/D is the ratio of xylem thickness to trunk diameter. Z ratio is the ratio of the section modulus calculated for the image with a hollow to that calculated for the solid image. The shape illustrated shows pattern IV with a hollow of 0.5 in terms of hollow/outside diameter ratio, i.e., a t/D ratio of 0.25

(0%–80% in hollow/outside diameter ratio) in a concentric configuration to that of the outside shape were made with image processing software. Then Z values were calculated from Eq. 9 using the bitmap images. The ratios of Z values for hollows of various sizes to that of the solid shape for the patterns I–IV are shown in Fig. 9, where the difference between the outside diameter and hollow diameter was defined as the twice of the xylem thickness. The Z ratios agreed well with the solid curve, which was calculated for the section modulus of a circular tree trunk with a hollow (Z_H) using Eq. 11:

$$Z_H = \frac{\pi}{32}\left\{\frac{D^4-(D-2t)^4}{D}\right\} \quad (10)$$

$$\frac{Z_H}{Z_S} = 1-\left(1-\frac{2t}{D}\right)^4 \quad (11)$$

where Z_S is the section modulus of a solid circular shape, D is the diameter of a circular-shaped trunk, and t is the thickness of the xylem.

The reduction in Z is calculated to be less than 5% when the xylem thickness is 26.4% or more of the trunk diameter. That is to say, the Z values of trunks that are hollow inside can be evaluated using the profile method together with the drill resistance technique on the condition that 26% of the trunk diameter could be drilled without skew.

Conclusions

1. Nondestructive estimation of the cross-sectional shape of tree trunks using a profile method was proposed. The section modulus of a cross section could be calculated from a generated binarized image.
2. The error in estimation of the section modulus of a tree trunk may be large for trunks with an irregular outside shape or a large diameter. Because of the cumulative

error that accompanies an increase in the number of gauge points, a long profile gauge is recommended for use on large diameter trunks.

3. The deviation of the needle of the drilling device (IML-RESI F500) caused by skew was found to be less than 20 mm at a depth of 210 mm; the error in the measurement of xylem thickness would thus be negligible. The Z values of hollow trunks can be evaluated using the profile method together with the drill resistance technique on the condition that 26% of the trunk diameter could be drilled without skew.

Acknowledgments The authors thank Mr. Masafumi Inoue for his kind assistance in the experimental work. This study was supported in part by JSPS KAKENHI (21580169).

References

1. Peters M, Ossenbruggen P, Shigo A (1985) Cracking and failure behavior models of defective balsam fir trees. Holzforschung 39:125–135
2. Mattheck C, Kubler H (1995) Wood – the internal optimization of trees. Springer, Berlin
3. Koizumi A, Hirai T (2006) Evaluation of the section modulus for tree-stem cross sections of irregular shape. J Wood Sci 52(3): 213–219
4. Habermehl A (1982) A new non-destructive method for determining internal wood condition and decay in living trees 1. Arboric J 6:1–8
5. Watanabe N (2000) Instruments available for tree diagnosis in the field (in Japanese). J Tree Health 4:23–32
6. Arita K, Mitani S, Sakai H, Tomikawa Y (1986) Inspection of internal decay in wooden poles using ultrasonic wave (in Japanese). Wood Ind. 41:370–375
7. Iizuka Y (2007) Wood-decay diagnosis system (in Japanese). Tree Forest Health 11:135–139
8. Rinn F, Schweingruber F-H, Schär E (1996) Resistograph and X-ray density charts of wood: comparative evaluation of drill resistance profiles and X-ray density charts of different wood species. Holzforschung 50:303–311
9. Yada S (2001) Inspection and repair of exterior wood (in Japanese). Wood Ind 56:452–457
10. Fujii Y, Fujiwara Y, Harada M, Kigawa R, Komine Y, Kawanobe W (2009) Evaluation of insect attack in wooden historic buildings using drill resistance method (in Japanese). Hozon Kagaku 48:215–222
11. Yamashita K, Nagao H, Kato H, Ido H (2006) Estimating variations in wood density by drilling resistance (in Japanese). Bull FFPRI 5:61–68